INTERPRETING RANGER PHOTOGRAPHS FROM IMPACT CRATERING STUDIES

By Donald E. Gault, William L. Quaide,
and Verne R. Oberbeck

National Aeronautics and Space Administration
Space Sciences Division
Ames Research Center, Moffett Field, California

ABSTRACT

Impact cratering experiments have been performed at the Ames Research Center and field studies of missile impact craters have been carried out at White Sands Missile Range, New Mexico. The studies show that projectiles with velocities typical of secondary bodies on the moon produce craters with geometries which are sensitive to target strength and angle of impact. The principal conclusion obtained from the application of the findings to the interpretation of Ranger photographs is that the lunar surface consists of materials of low cohesive strength. The thickness is not certainly known, but it is probably measured in meters or tens of meters.

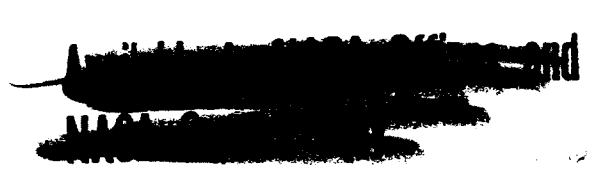

INTRODUCTION

Cratering experiments at the Ames Research Center and field studies of missile impact craters at White Sands Missile Range, New Mexico, have provided information which is of great value for interpreting Ranger photographs. Before considering the evidence and interpretations, it is necessary to point out that the experiments were performed by means of projectiles with velocities in the 1 km/sec range. It is known from earlier work that the geometry of craters produced by hypervelocity impact is insensitive to material strength of the target and independent of incidence angle of the projectile. Recent studies have shown, however, that target strength is an important parameter in determining the geometry of a crater produced by a low velocity impact. The purpose of this paper is twofold. First, experimental evidence is presented which shows the relationship between such parameters as target strength, projectile velocity and angle of impact, and the resulting crater geometry. Secondly, the results of the studies are used to interpret the properties of the lunar surface by considering the geometry of craters of probable secondary (low velocity) origin seen on the Ranger photographs.

Secondary is used here in a genetic sense to indicate an origin from low velocity projectiles created by an impact of a primary, extra-lunar body. It is not used in a morphological sense as is done by Shoemaker (this symposium). The results of our work indicate that secondary craters cannot be distinguished from primary craters on the basis of geometry alone.

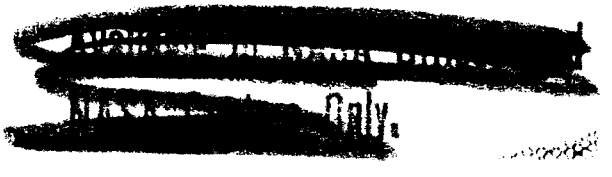

EXPERIMENTAL EVIDENCE

The experimental facility, the vertical gun, used to obtain most of the evidence presented here, is shown in figure 1. It consists of an A-frame which straddles a large vacuum tank. The gun rests on a boom. The boom can be raised so that the gun can fire into the target medium inside the vacuum chamber at various angles from the horizontal to the vertical in 15° increments. The pressure inside the chamber at the time of impact is of the order of 100 microns of mercury.

Target materials used to date are loose sand, bonded sand, clastic pumice debris, pumice blocks, and two layer models of pumice blocks overlaid by clastic pumice debris. Impacts into loose sand and pumice debris produce craters which are circular in plan regardless of the angle of impact. The craters are surrounded by a raised rim, characteristic rays, and granular ejecta. Impacts into sand which has small amounts of binder produce craters which differ strongly in geometry, morphology, and size. Figure 2 graphically illustrates this point. The two craters shown were formed under identical conditions, except that the one at the top was produced in bonded sand whereas the one at the bottom was noncohesive. The binder is Portland cement, one part in 40 parts sand. The unconfined compressive strength of the bonded material is about 10^6 dynes/cm^2 and crumbles very easily between the fingers. The angle of impact (from the horizontal) was 30° in both cases. The projectiles were aluminum with velocities of approximately 1 km/sec. The craters differ in both morphology and size. The crater in unbonded sand is circular in plan, whereas the crater in the

bonded sand is elongate in plan. The character of the ejecta and the morphology of the crater rims are strikingly different. The rim of the crater in bonded sand is poorly developed and contains numerous blocks of ejecta. The rim of the crater in loose sand is strongly developed and smooth. Ray systems are developed in both cases. It was found that the ray system produced under a given set of experimental conditions provides information regarding the angle of impact of the projectile. Figure 3 illustrates this very graphically. The target material in this experiment was poorly sorted fragmental pumice with a bulk density of 1.1 g/cc. The impact velocity was 1 km/sec and the projectiles were composed of lexan, a plastic. Impacts with incidence angles of 90°, 60°, 30°, and 15° from the horizontal are shown. The projectiles entered from the left in all oblique cases. The ray system produced by the normal impact is strikingly symmetrical. Oblique impacts focus the ray patterns, the focusing being very pronounced in the case of shallow impact angles. It must be emphasized, however, that projectile velocity, projectile density, and target strength also have an effect on the degree of focusing of the ray ejecta, the details of which remain to be worked out.

Another geometrical feature of the craters has been observed which is related to the degree of obliquity of the impacting projectile. This feature is the shape of the crater in profile in the direction of the projectile trajectory. At low entry angles, 30° and below, the crater wall is steeper on the side from which the projectile enters the target. The asymmetry in profile is revealed by shadow shapes when incident light is at a large angle to the line of the projectile trajectory. This feature is demonstrated in

figure 4. The crater shown in the two photographs was produced by a projectile with a velocity of 1 km/sec impacting an unbonded sand target at an angle of 15° from the horizontal. The crater is circular in plan but asymmetric in cross section. The two photographs were taken with the incident light parallel and at right angles to the projectile trajectory. The shadow pattern is asymmetrical when the incident light is at right angles to the line of flight, revealing the asymmetry of crater profile. Many such shadow patterns can be seen on the Ranger photographs. These, combined with focused ray patterns, provide a powerful tool for identifying the direction from which crater-producing secondary bodies came. Figure 5 summarizes the change in crater profile with angle of incidence for craters produced in unbonded sand by lexan projectiles with velocities of 1 km/sec. Shown also is displaced mass and crater diameter. At 90° the crater is roughly conical with a raised rim; at 60° the shape is nearly the same; at 30° the crater wall on the projectile entry side is noticeably steeper; and at 15° the profile asymmetry is even more pronounced. Displaced mass is a factor of 40 greater than that produced previously by impacts of the same energy in cohesive or massive rock targets; it decreases very quickly with decreasing angles of impact. At angles of 30° ricochet sometimes takes place, whereas at 15° it always occurs.

Experiments have been performed with pumice blocks and two-layer models of pumice blocks overlaid by granular pumice debris. Results are shown in figure 6 for impacts of lexan projectiles with velocities of 1 km/sec. A normal impact into a pumice block with a density of 0.6 - 0.7 g/cc is shown at the upper left. Such an impact produces a cylindrical hole with a diameter only minutely larger than that of the projectile and 10 to 12 cm

deep. An oblique impact into the same material is shown at the upper right. A simple elliptical groove is produced. The two lower photographs are of layered targets. Both are composed of machined pumice blocks overlaid by varying thicknesses of granular pumice fragments. The crater at the lower left was produced by a projectile traveling at an angle of 30° from the horizontal and impacting a target with a surface layer 1.5 cm thick, a thickness less than the diameter of the 20-mm projectile. The crater is circular in plan but has a flat floor where the fragmental materials were cleared from the rock surface. The center of the crater is occupied by a deep cylindrical hole. The target on the lower right has a surface layer 4 cm thick. The crater depth in this model is exactly the same as though the pumice rock were not present. There is only a vague indication of crushing of the block at the bottom of the crater. Much experimentation remains to be done with layered models, but the preliminary information presented here certainly has a bearing on the current interpretation of Ranger photographs.

One other observation which may be of value for interpreting Ranger photographs is the occurrence of slumps in some of the craters with surface textures similar to the tree bark texture observable on all high resolution Ranger photographs. An example is shown in figure 7. This crater was produced in loose sand by a 30° impact of an aluminum projectile with a velocity of 1 km/sec. The texture is the result of post cratering slumping of finely crushed quartz. The same kind of texture has been observed in impact craters produced in 15-micron-diameter particulate material. It is possible that the tree bark texture visible on the high resolution Ranger picture is not a lava surface feature but instead is a result of slumping.

There is always a question of how well the small laboratory craters can be compared with larger lunar counterparts. Relevant information is being gathered in a program of field studies of craters produced by the impact of unarmed missiles at White Sands Missile Range, New Mexico. The craters studied are of the same size as those visible on the higher resolution Ranger photographs. One such crater is shown in figure 8. The angle, velocity, and energy of the impacting missile are known. The velocity is typical of a lunar secondary impact. The target material is a strongly cemented gypsiferous sand. The crater is elongate with a length to width ratio of 2. The projectile entered from the right. The crater shape and the ejecta distribution are both asymmetric. One large block is visible on the crater rim. This view also shows very clearly the focusing of the ejecta.

Missiles with the same entry angles, velocity, and energy produce significantly different craters when they impact weakly cohesive materials. Figure 9 is a photograph of a crater in very weakly cohesive material. The crater, produced by a missile entering from the left, is 10 meters in diameter and is almost perfectly circular. Figure 10 shows another crater of similar size produced in weakly to noncohesive material. It is circular in outline and again block ejecta is rare. The one large block visible was produced by shock compression and was not a part of the original target material. It is extremely weakly bonded, so weak that it can not be picked up. Impact craters produced in very strong rock targets are significantly different. They are of irregular shape with hardly any rim and have abundant large blocks of ejecta.

Field studies thus confirm the results obtained in the laboratory. Circular craters are produced by low velocity impacts in weakly to noncohesive materials regardless of the angle of impact. Impacts in cohesive materials produce craters which are asymmetric in plan and surrounded by blocky ejecta. Figure 11 shows the plan outlines of a number of craters at White Sands, New Mexico, along with a qualitative description of the degree of cohesiveness of the impacted materials. Impacts in very strongly cohesive rock targets produce irregularly shaped rimless craters with a profusion of large ejecta blocks in and around the crater.

One other result of the White Sands study presents evidence which bears on the problem of identification of secondary craters. Figure 12 is a map of the ejecta of a White Sands Missile Range impact crater prepared by Dr. Henry Moore of the U. S. Geological Survey. The features to be observed are the patterns exhibited by the secondary impact craters produced by low strength ejecta clots. All imaginable patterns can be observed, random, clusters, straight radial lines, straight lines which are not radially directed, and looping lines. The secondary craters are all small but are of various shapes. All were produced by very low-speed projectiles with velocities of meters per second. Some of the impacting projectiles remained intact in the crater. These impacts were nonviolent in that the clots of material did not break up and were not thrown free of the crater. Other craters must have been produced by projectiles of about the same ejection and impact velocities, but the clots were weaker and broke apart. The shapes of these craters are functions of both the strength of materials and impact velocities. The details of their geometry cannot be compared directly with the geometry of secondary

lunar craters produced by projectiles with velocities of kilometers per second. The cratering process in the latter case is significantly different; however, the distribution pattern can be used. The pattern suggests that secondary craters on the moon may occur randomly, in which case they may not differ sufficiently in geometry to distinguish them from craters produced by primary bodies. They may also occur in clusters or linear arrangements. Such arrangements are not suspected for primary bodies and it is on this basis only that secondary craters may be identified. Even this criterion is subject to error because of the fact that volcanic craters most frequently occur in clusters and linear arrangements.

INTERPRETATION OF RANGER PHOTOGRAPHS

The physical characteristics of the lunar surface can be interpreted from the Ranger photographs using the results of the low velocity cratering studies only when low speed (secondary) impact craters can be identified. It was stated earlier that the geometry of craters produced by primary and secondary projectiles may not be sufficiently different to be distinguished. Craters of secondary origin can be identified unequivocally only when they occur in clusters or in linear arrays within ray patterns emanating from prominent craters or when focused ejecta patterns and asymmetric shadow patterns indicating cross-sectional asymmetry can be seen.

On the basis of the above evidence, secondary craters can be identified on Ranger VII and VIII photographs. Ranger VII impacted in an area traversed by rays from the craters Copernicus and Tycho. Figure 13 is a Ranger VII, A-camera photograph showing a cluster of craters (near the top of the

photograph) from which an ejecta plume extends generally northward. The direction of the plume lines up exactly with a line through the source craters to Tycho. The same cluster of craters appears in a closer view in the upper left corner of figure 14. Since rays from Tycho do extend through the area and the ejecta plume does line up, it is most likely that the cluster was produced by blocks thrown from Tycho. The acute angle formed by the plume suggests that the projectiles struck the surface at low angles from the horizontal, probably in the neighborhood of 15° to 30°. This angle, together with the distance from Tycho, suggests that the impact velocity was of the order of 1.3 km/sec.

Another cluster can be seen a few tens of kilometers to the southeast. This cluster has generally been considered to have been produced by impacts of secondary bodies from Tycho. There is doubt that ejecta plumes can be unequivocally linked with these craters, but there is no doubt that asymmetric shadow patterns are present in some of the craters and that the steep slope is on the side of the crater closest to Copernicus. In keeping with experimental evidence, it is proposed that this cluster of craters had its origin by low angle impacts of secondary bodies derived from Copernicus. The fact that the craters are predominantly circular in plan indicates that the surface is composed of materials which are at least weakly cohesive. The weakly cohesive layers must extend to a considerable depth. Many of the craters of the cluster are well-formed, bowl-shaped structures having no geometrical features indicative of a two-layer model where the upper layer is thin relative to the crater depths observed (30-150 meters).

Ranger VIII photographs contain similar evidence. The Ranger VIII spacecraft traversed a large portion of Mare Tranquillitatis, a region where the surface is crossed by many prominent rays emanating from the crater Theophilus. Figure 15 is a photograph showing one of the more prominent rays. The higher density of craters within the ray, the linear chains of some craters in the ray, and the asymmetric shadow patterns all support the concept that these craters were produced by low angle impacts of secondary projectiles from Theophilus. Figure 16 is a view of the region slightly to the south of that shown in figure 15. Elements of the same ray can be seen (A). Other rays of probable Theophilus origin can be observed and at least one of probable Tycho origin is present. In addition to the rays, a few gouges can be seen (B). Others can be seen on other photographs. Ricochets were observed in the laboratory in low angle, low velocity experiments where the projectiles have grooved the surface near the crater in an irregular manner. The grooves observed may well result from such projectile behavior.

If craters in the ray systems are produced by secondary projectiles as proposed, and if the number of randomly distributed secondary craters is as great as size-frequency plots of the craters suggest, the prevalence of circular craters and the rarity of positive relief features on Ranger VIII photographs suggest that surface materials in this area are weakly cohesive. The thickness must be measured in meters or tens of meters to account for the geometry of the larger secondary craters.

In view of the foregoing conclusions it is necessary to explain the variety of crater forms observed on the Ranger photographs. It is suggested that the continuum of crater forms observable from sharp, well defined ones

to faint, shallow, hardly recognizable ones was not the result of different mechanisms of formation but instead was produced by modification of the craters. It must be remembered that impact does not clean the surface; it litters the surface. Each high-speed impact excavates a thousand or ten thousand times the mass of the incoming projectile. Of this only an amount equal to a few projectile masses leaves the moon. The rest is spread over the surface and must modify previously existing topographic features, preferentially eroding positive relief features and covering all with ejecta. The deposited material is thickest in depressions, but the whole of the surface is blanketed. The inevitable result of this process repeated again and again is the production of a continuum of crater shapes.

Photographs from the Ranger IX mission have provided new and different information to be considered in an interpretation of the lunar surface properties. These photographs indicate that the floor of the crater Alphonsus has not only been bombarded by projectiles but that a significant amount of the surface detail has been created by explosive outgassing from vent craters. Details of the surface suggest that the products of this activity, probably volcanic, are clastic blankets with physical properties similar in all respects to impact ejecta deposits. Collapsed craters appear to be present as well. It is not known if such explosive outgassing activity is restricted to certain large craters or if it has been widespread on the maria surfaces. If it has occurred on the maria the thicknesses of fragmental material suggested by this investigation may be more readily understood than if the ejecta had been formed by impact alone.

CONCLUSIONS

Experiments indicate that the geometry of craters produced by hypervelocity impact is generally insensitive to the strength of the target material and angle of impact. The geometry of craters produced by the impact of projectiles with velocities similar to those of secondary bodies on the moon is quite sensitive to target strength and angle of impact. Projectiles with these velocities produce circular craters in noncohesive materials regardless of the angle of impact and elongate or irregular craters in cohesive materials when the angle of impact is low. In addition, ejecta from noncohesive targets has a maximum block size equal to the maximum diameter of the components of the target, whereas ejecta from cohesive targets has a large range of sizes. Oblique impacts produce focused ejecta patterns and crater asymmetry in the plane containing the projectile trajectory, enabling identification of the direction of origin of the impacting body.

Secondary craters can be recognized on Ranger photographs when they occur in clusters or in linear arrays within well-defined rays, or when they have focused ejecta patterns and cross-sectional asymmetry. Analyses of such craters indicate that they are predominantly circular in outline, that there is an absence of ejecta with large diameters, and that their geometry is so regular that the lunar surface must be composed of weakly to noncohesive materials with thicknesses measured in meters or tens of meters. The surface materials may be composed entirely of impact ejecta or they may be of mixed origin, part impact and part explosive outgassing.

LIST OF FIGURES

Fig. 15.- Ranger VIII photograph showing a prominent Theophilus ray.

Fig. 16.- Ranger VIII photograph showing a portion of the ray of figure 15 and other ray elements.

A-33996

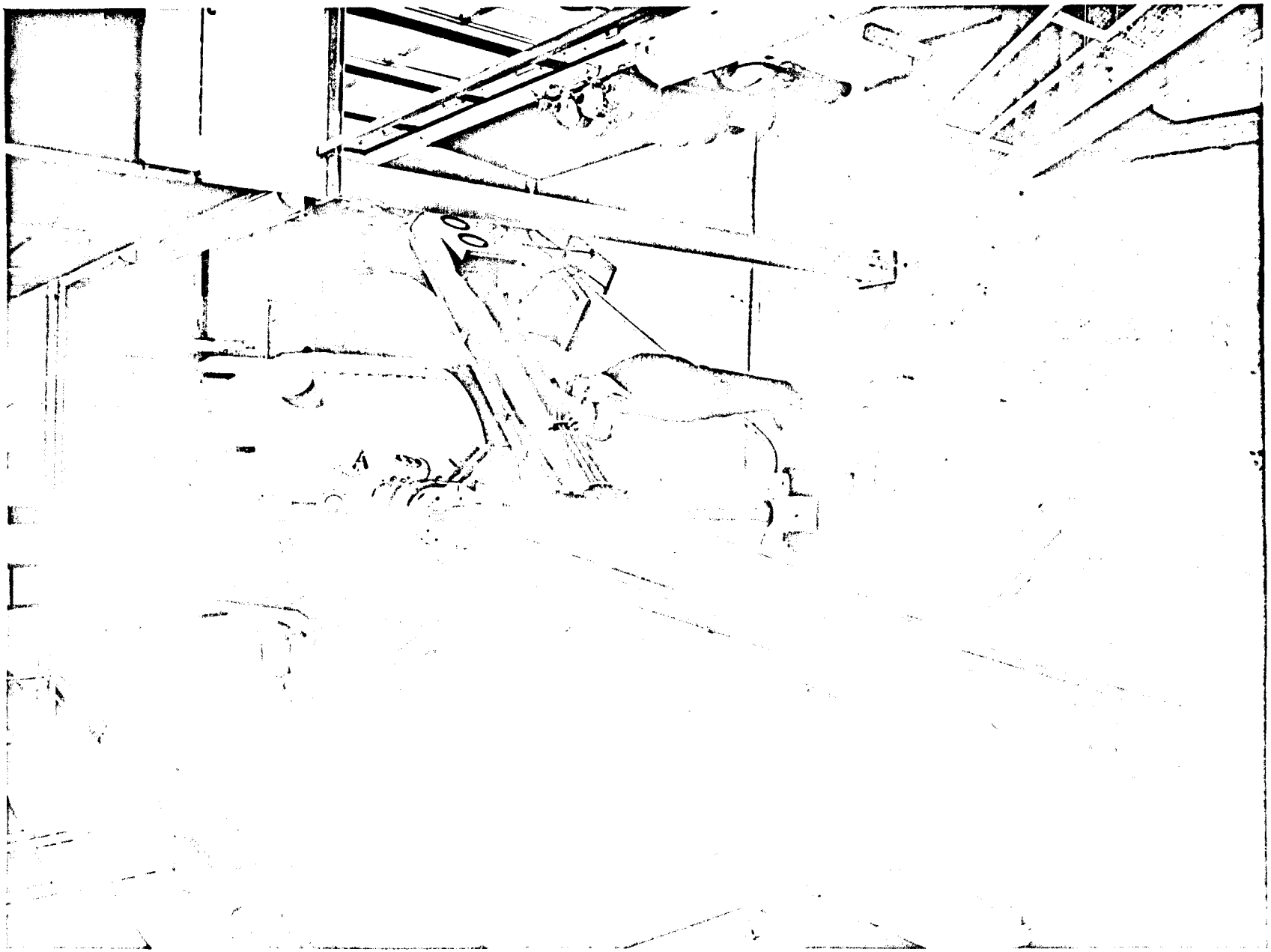

NATIONAL AERONAUTICS AND SPACE ADMINISTRATION
AMES RESEARCH CENTER, MOFFETT FIELD, CALIFORNIA

A-34298-1

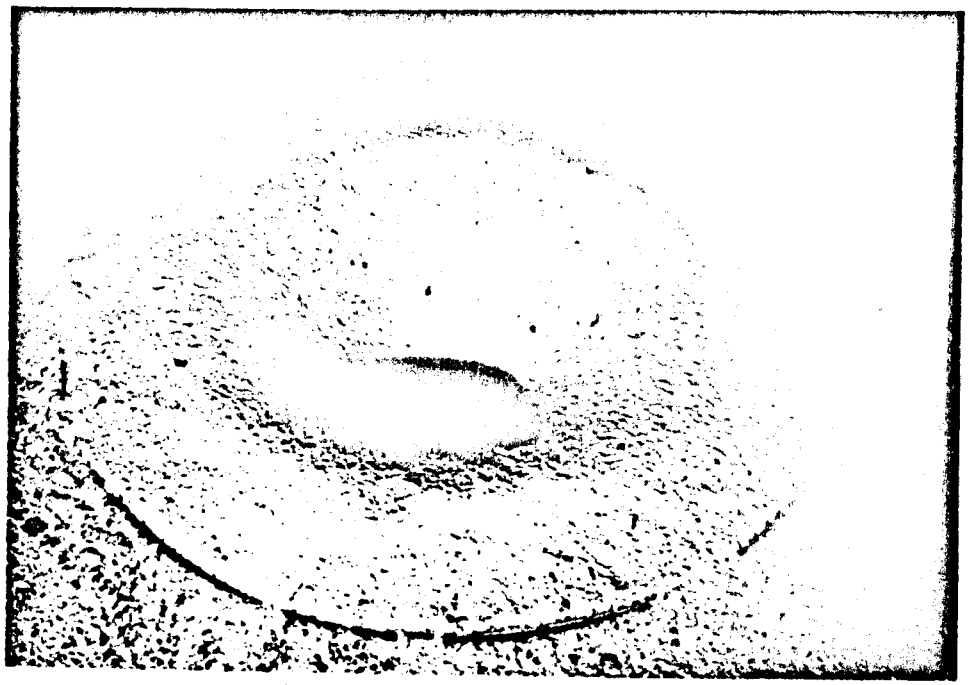

Fig. 2

NATIONAL AERONAUTICS AND SPACE ADMINISTRATION
AMES RESEARCH CENTER, MOFFETT FIELD, CALIFORNIA

A-34298-2

EJECTA PATTERNS
PUMICE

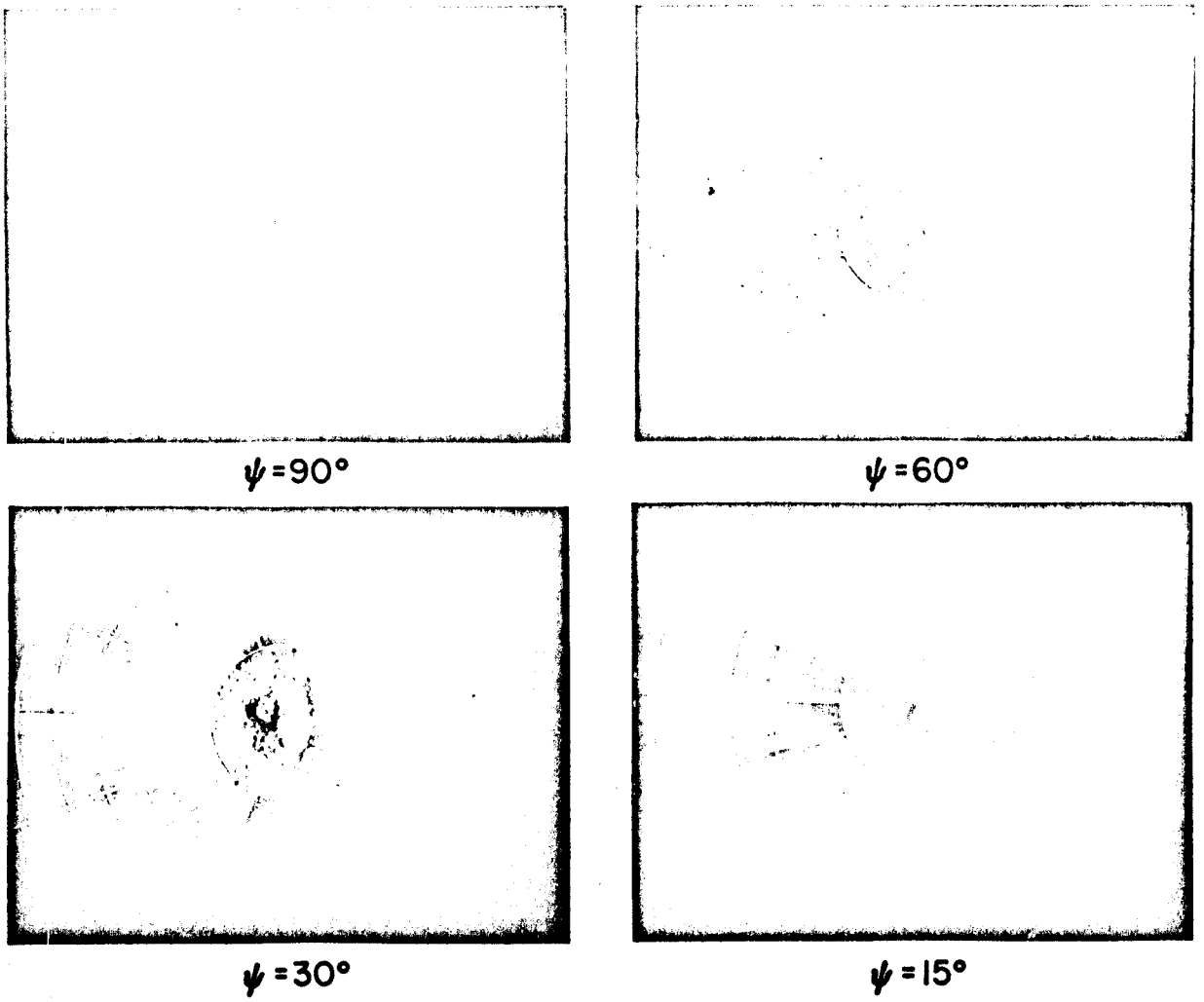

$\psi = 90°$ $\psi = 60°$

$\psi = 30°$ $\psi = 15°$

Fig. 3

NATIONAL AERONAUTICS AND SPACE ADMINISTRATION
AMES RESEARCH CENTER, MOFFETT FIELD, CALIFORNIA

A-34553-6

CRATER SHADOW PATTERNS
UNBONDED QUARTZ SAND, $\psi = 15°$

Fig. 4

NATIONAL AERONAUTICS AND SPACE ADMINISTRATION
AMES RESEARCH CENTER, MOFFETT FIELD, CALIFORNIA

A-34298-4

OBLIQUE IMPACT
UNBONDED QUARTZ SAND

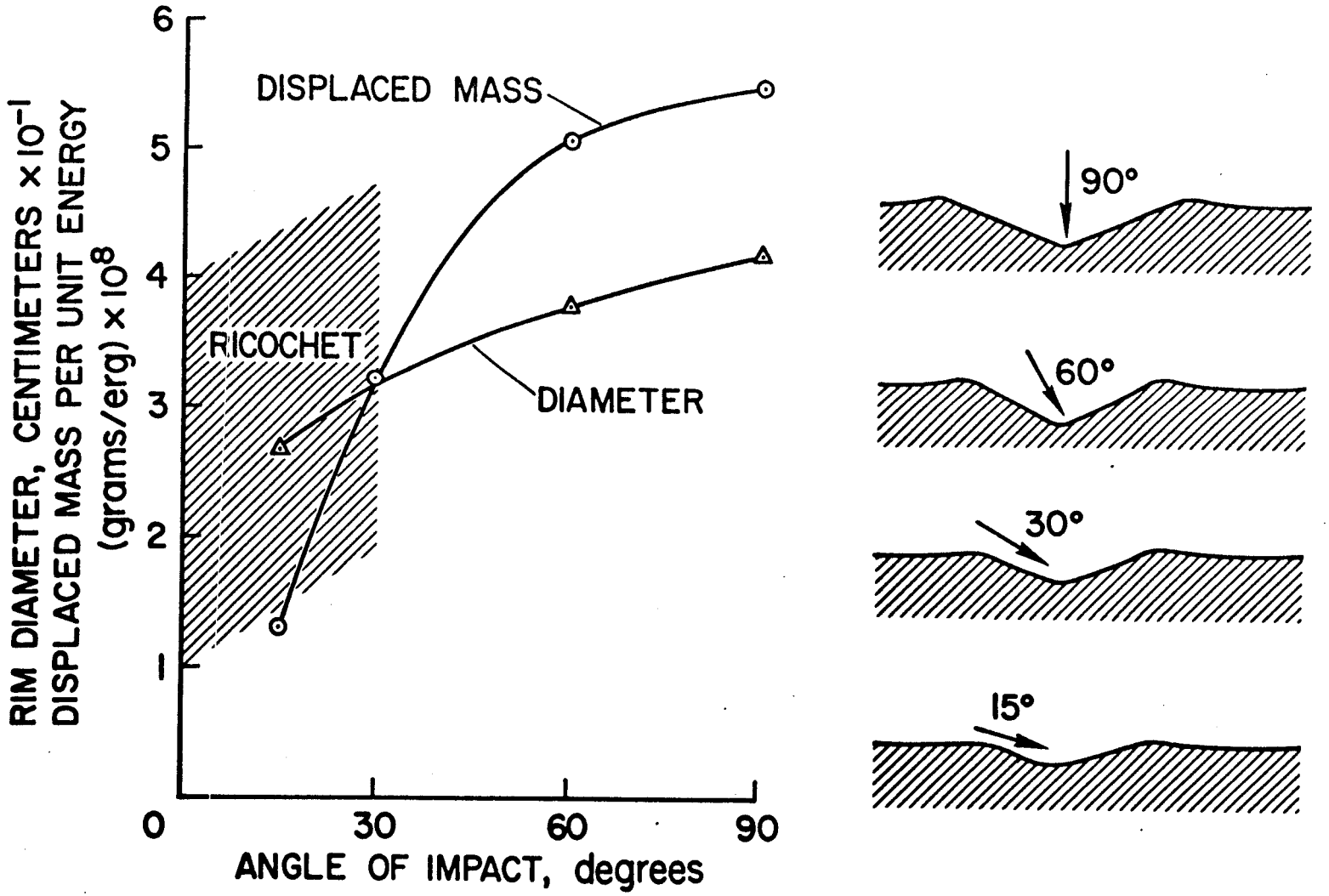

Fig. 5

NATIONAL AERONAUTICS AND SPACE ADMINISTRATION
AMES RESEARCH CENTER, MOFFETT FIELD, CALIFORNIA

A-34298-3

IMPACT IN PUMICE

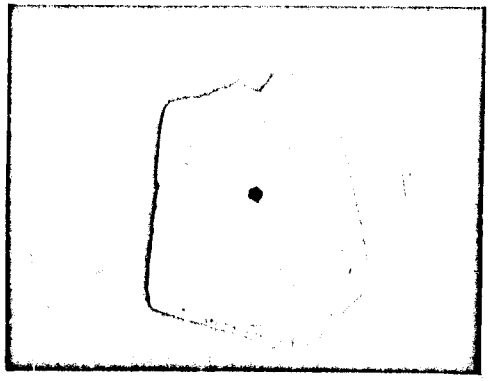

$\psi = 90°$

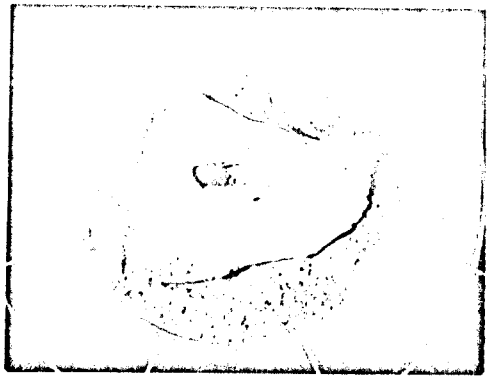

$\psi = 30°$

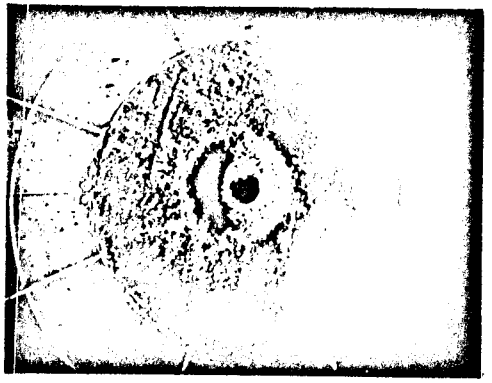

$\psi = 30°$, 1.5 cm PUMICE DUST

$\psi = 30°$, 4.0 cm PUMICE DUST

Fig. 6

NATIONAL AERONAUTICS AND SPACE ADMINISTRATION
AMES RESEARCH CENTER, MOFFETT FIELD, CALIFORNIA

A-34553-23

POST CRATERING MODIFICATION
SLUMPING

Fig 7

NATIONAL AERONAUTICS AND SPACE ADMINISTRATION
AMES RESEARCH CENTER, MOFFETT FIELD, CALIFORNIA

A-33453

USAF PHOTOGRAPH

Fig. 8

NATIONAL AERONAUTICS AND SPACE ADMINISTRATION
AMES RESEARCH CENTER, MOFFETT FIELD, CALIFORNIA

A-33774

Fig. 9

NATIONAL AERONAUTICS AND SPACE ADMINISTRATION
AMES RESEARCH CENTER, MOFFETT FIELD, CALIFORNIA

A-33454

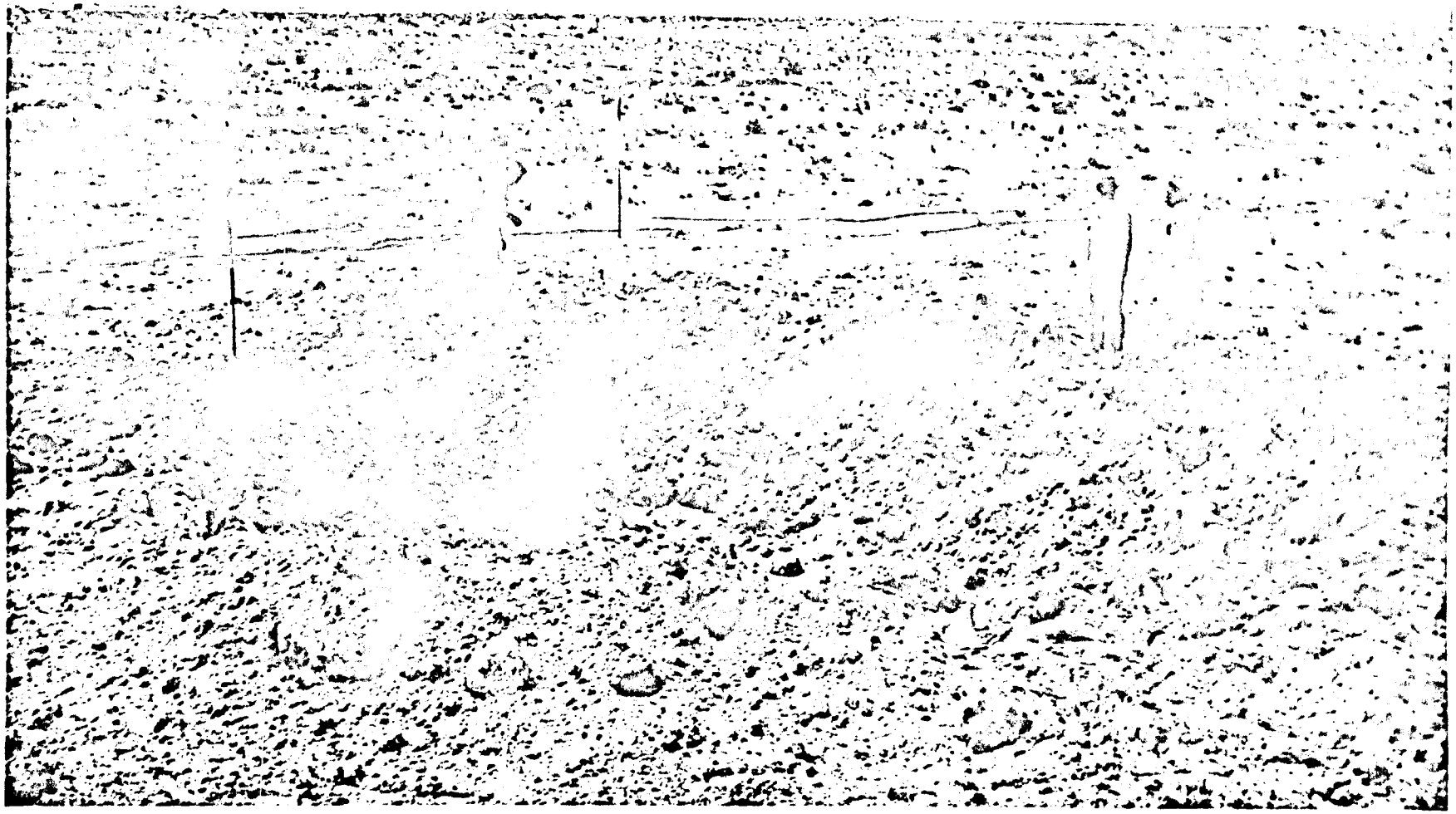

Fig. 10

NATIONAL AERONAUTICS AND SPACE ADMINISTRATION
AMES RESEARCH CENTER, MOFFETT FIELD, CALIFORNIA

WSMR IMPACT CRATERS

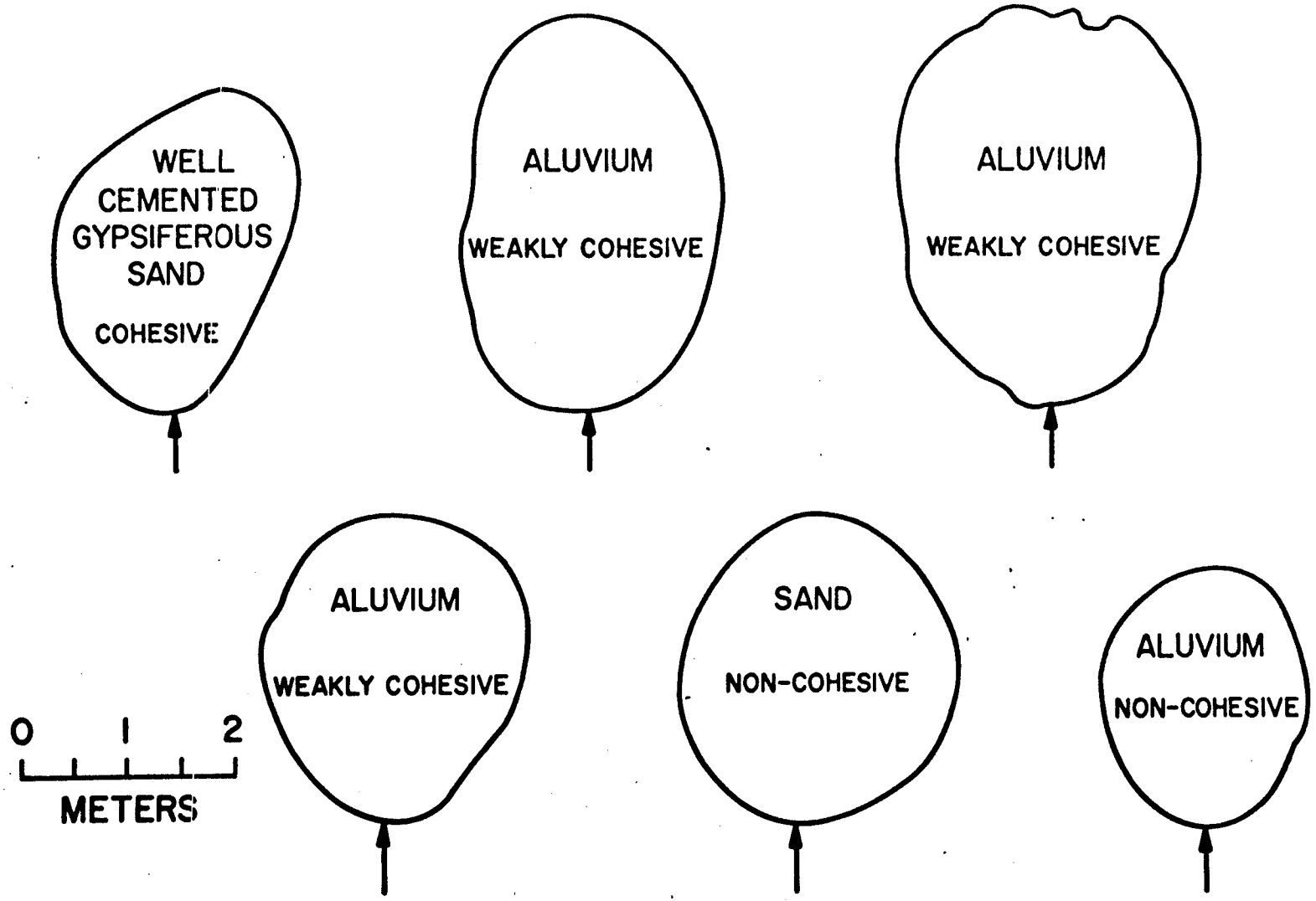

Fig. 11

NATIONAL AERONAUTICS AND SPACE ADMINISTRATION
AMES RESEARCH CENTER, MOFFETT FIELD, CALIFORNIA

A-34240-9

WSMR IMPACT CRATER

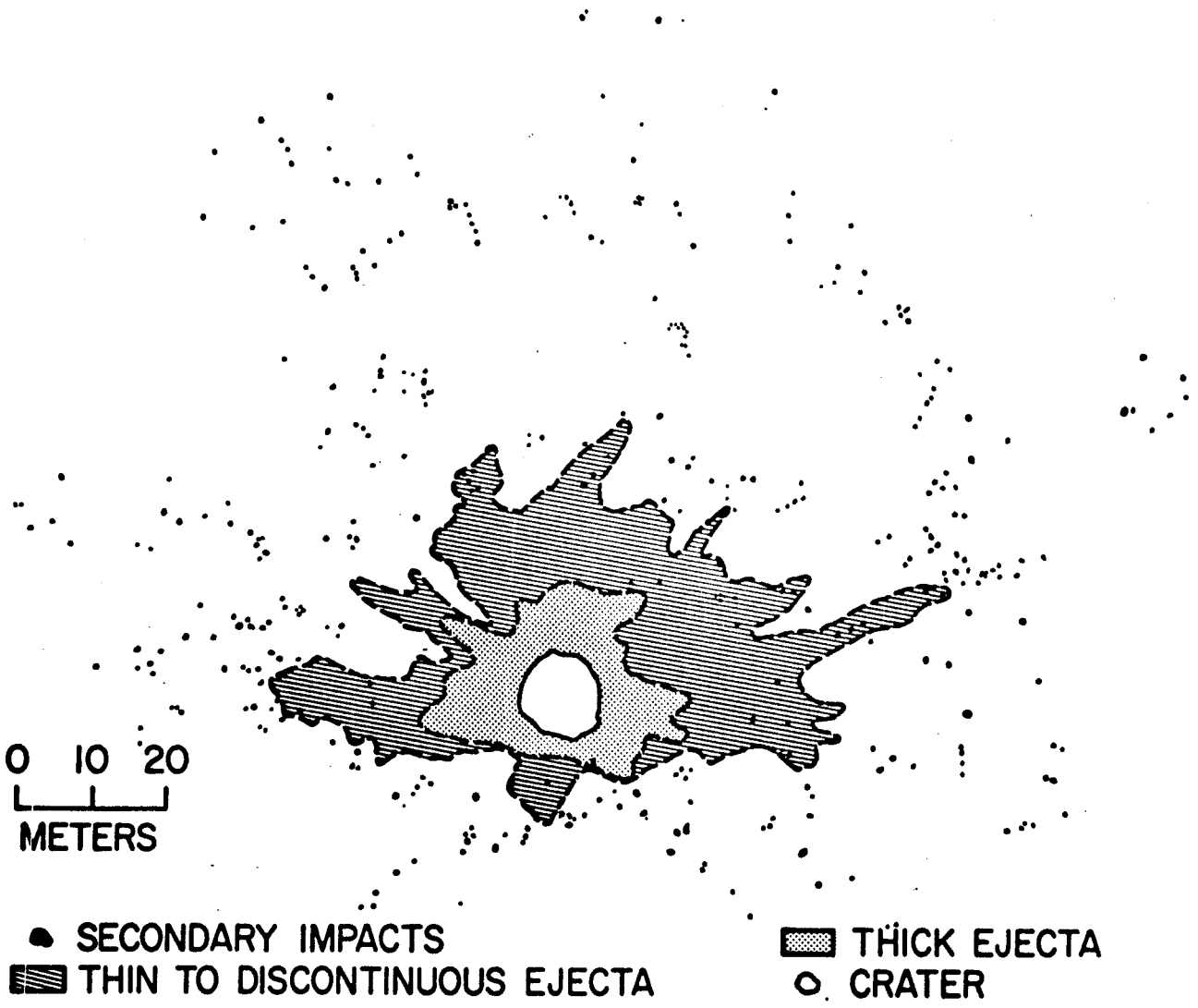

Fig. 12

NATIONAL AERONAUTICS AND SPACE ADMINISTRATION
AMES RESEARCH CENTER, MOFFETT FIELD, CALIFORNIA

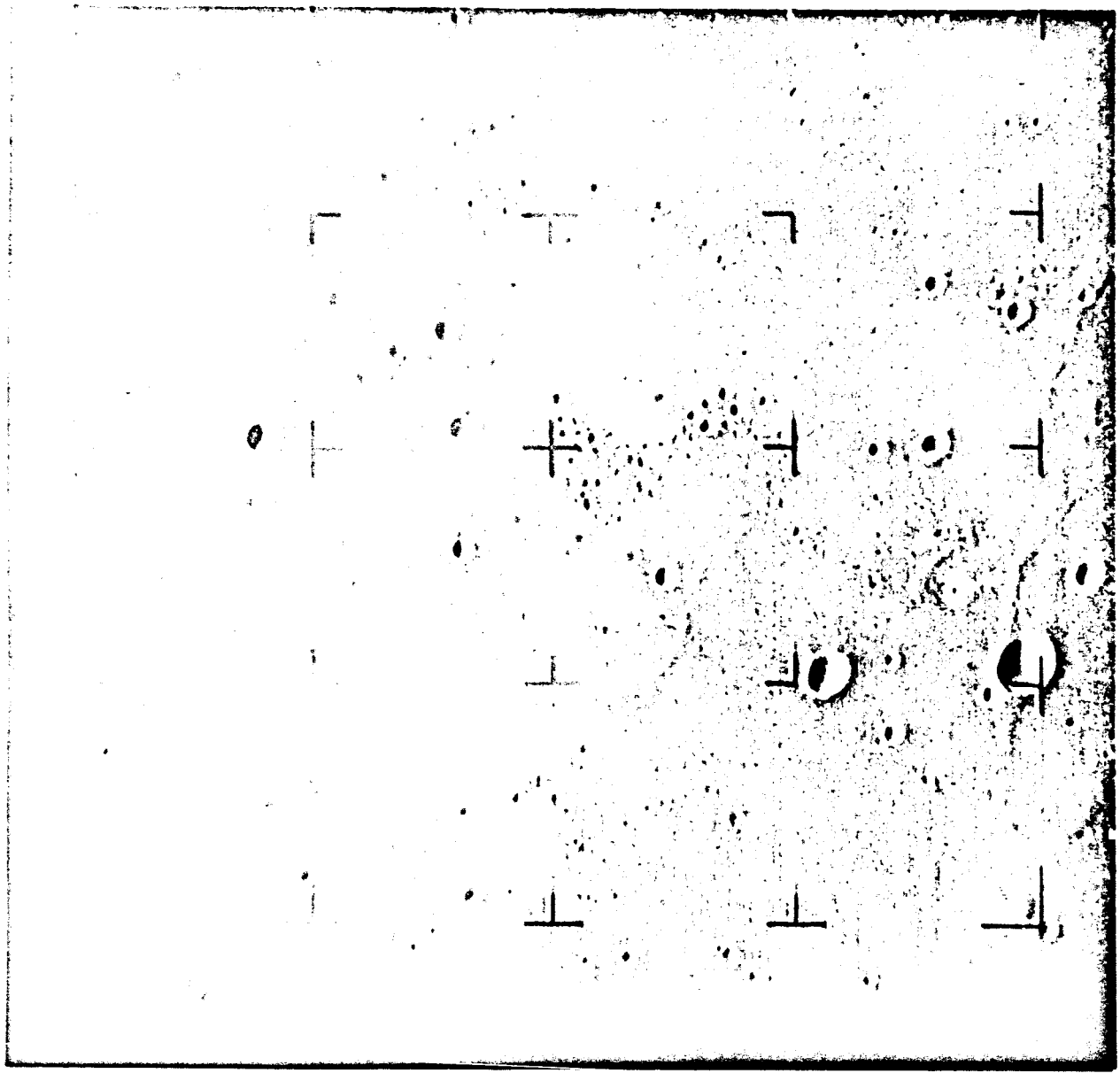

A-34553-13

Fig. 13

NATIONAL AERONAUTICS AND SPACE ADMINISTRATION
AMES RESEARCH CENTER, MOFFETT FIELD, CALIFORNIA

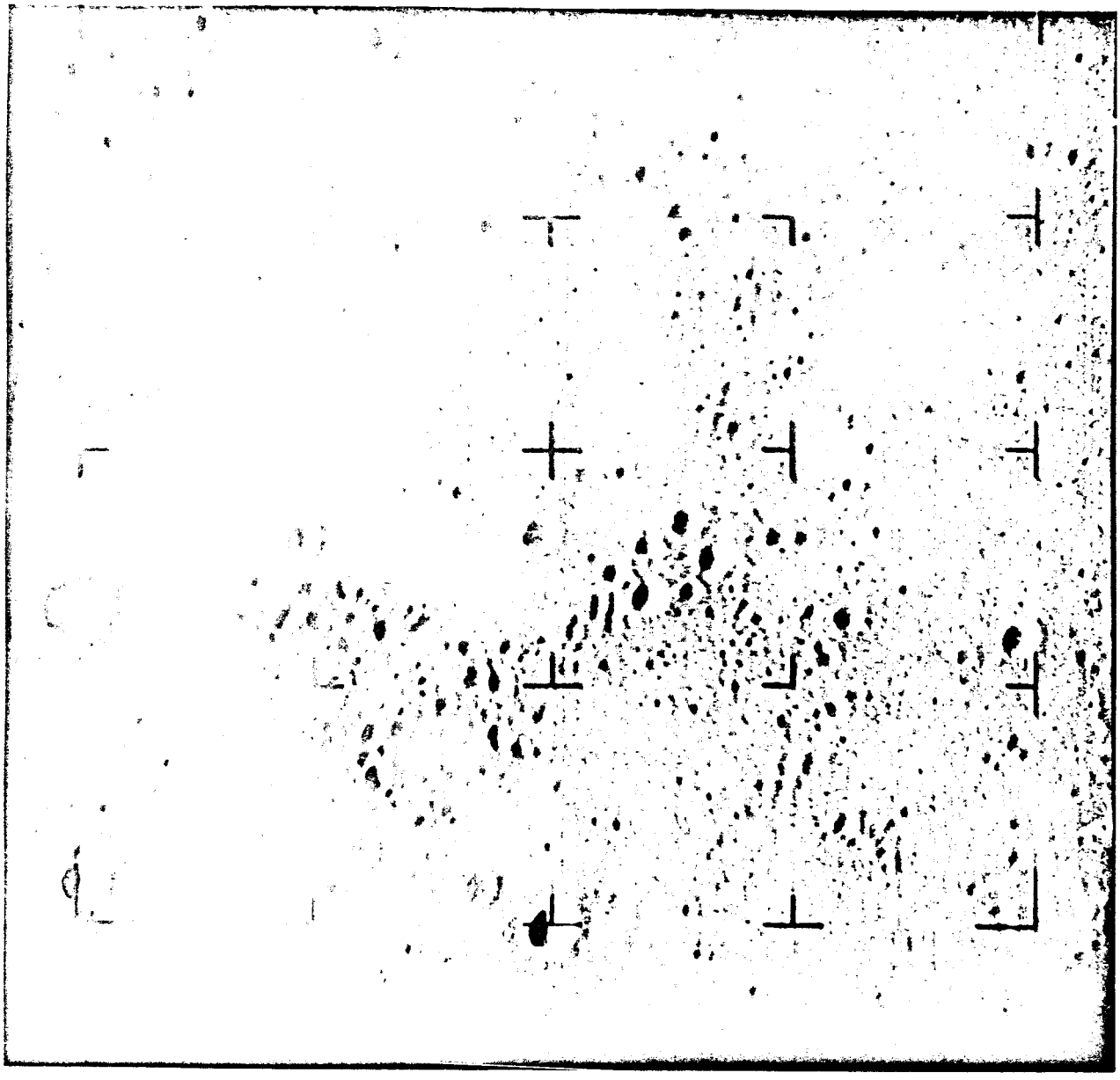

A-34553-14

Fig. 14

NATIONAL AERONAUTICS AND SPACE ADMINISTRATION
AMES RESEARCH CENTER, MOFFETT FIELD, CALIFORNIA

Fig. 15

Fig. 16